We H 03

Effects of Clay Swelling or Shrinkage on Shale Caprock Integrity

R. van Noort* (Institutt for Energiteknikk)

Summary

During CO2 injection and storage, the exposure of shale caprock to dry supercritical CO2 can lead to clay dehydration and shrinkage. This has been proposed as a potential leakage risk for shale caprocks during CO2 storage. We report permeability measurements on pressed tablets of smectite and a smectite-quartz mixture, aimed at directly observing the effects of mineral composition, confinement, hydration, and exposure to CO2 on the permeability of clay-rich materials. Our results indicate that confinement and mineral composition have a strong impact on permeability. Furthermore, hydration always lead to a decrease in CO2-permeability, which varied from less than one to several orders of magnitude depending on sample mineral composition and confinement. Exposure of a hydrated sample to (a flow of) dry supercritical CO2 did not result in a long term increase in permeability, as might be expected as a result of dehydration-induced shrinkage. Subsequent drying of the hydrated samples at elevated temperature outside the vessel did result in a return of permeability to the original dry values. When combined, our results suggest that clay shrinkage is not a significant CO2 leakage mechanism in shale caprocks, though further tests, including longer exposure to a flow of supercritical CO2, are required.

Introduction

Shales make up an important caprock over many reservoirs targeted or already used for CO_2-injection and storage. The integrity of this shale caprock commonly is the main factor determining whether CO_2 can be stored safely over a long period, or whether leakage will occur. An important tool for assessing caprock integrity is through permeability measurements, preferably performed under in-situ conditions (e.g., Dong et al. 2010, Chalmers et al. 2012, Ghanizadeh et al. 2015, Van Noort and Yarushina, 2016). Such measurements have shown the effective confining pressure to be an important control on shale permeability. However, these measurements are often carried out using inert gases such as argon (Ar) or helium (He), and do not take into account possible interactions between clay minerals in the shale, (pore) water, and injected CO_2.

Certain clay minerals, such as smectite, swell when absorbing water and shrink when drying. Wang et al. (2014) showed both hydration and dehydration to induce the formation of microcracks in 1 mm thick slices of argillaceous rock, as a result of swelling and shrinkage under unconfined conditions. Studies on unconfined samples consisting of smectite (Schaef et al. 2012, Ilton et al. 2012, De Jong et al. 2014) have further shown that exposure to (supercritical) CO_2 can cause smectite either swell through absorption or shrink through dehydration. Based on these observations, Schaef et al. (2012) suggest that exposure to CO_2 and subsequent clay dehydration and shrinkage may lead to increases in caprock permeability. Ilton et al. (2012) more conservatively suggest this may only take place at defects (such as fractures) initially present in the shale caprock. Busch et al. (2016) argue that such effects would be limited to leakage along the injection wellbore. In addition, the impact of smectite swelling or shrinkage on caprock permeability may also depend on the shale mineral composition, its microstructure, and on the confining stress conditions.

We report experiments directly addressing the effects of shale mineralogy, clay swelling and confinement stress conditions on the permeability of analogue shale samples.

Method

In this study, we performed experiments addressing the effects of mineral composition, smectite swelling and stress conditions on shale permeability. The experiments were performed analogue samples, in form of pressed tablets consisting of smectite (SAz-1 "Cheto" Ca-montmorillonite) or mixtures of smectite and quartz. These tablets were prepared by mixing pre-weighed powders of individual minerals, and then loading these into a hand-operated tablet press with a 25mm circular die, and pressing them at ~45 MPa for 5-10 minutes. Sample 4 was pressed at ~125 MPa.

Different confinement conditions, labelled "dynamic" and "passive" confinement were achieved by either jacketing the sample in FEP, allowing for a transmission of confinement stress and the swelling of the sample (dynamic), or by directly pressing the tablet into a thick-walled stainless steel ring with an outer diameter of 25mm, so that confinement stress was not transmitted, and in turn the sample could not expand beyond the ring (passive). A list of all samples is given in Table 1.

Table 1 *Samples prepared and studied in this research.*

Sample #	Composition (g/g)	Mass (g)	Density (g/cm^3)	Notes
2	Sm	4.881	1.60	Inside steel ring; dry, wet; Ar, CO_2
3	Sm		1.90	Dry, wet; Ar, CO_2
4	0.69 Q; 0.31 Sm	12.474	2.06	Dry, wet; CO_2

Permeability measurements were performed on these samples in a purpose-built permeameter, allowing for both transient pulse and constant flow type measurements under effective confinement, and at controlled temperature (see Figure 1). To prepare a series of measurements, a sample was first placed between two grooved, bored pistons and hastelloy porous plates. This piston-sample assembly was jacketed in heat-shrink FEP, and built into the apparatus. Next, the confining and pore pressures were increased in steps, always ensuring that the confining pressure was higher than the pore pressure, and that the difference (the effective confining pressure) was lower than the planned effective confining pressure for the first measurement. Once the sample pressure and temperature stabilized, an individual pulse measurement was started by starting the data logger, and then quickly increasing the upstream pressure. The permeability was calculated from the gradual decrease of the upstream pressure and increase of the downstream pressure.

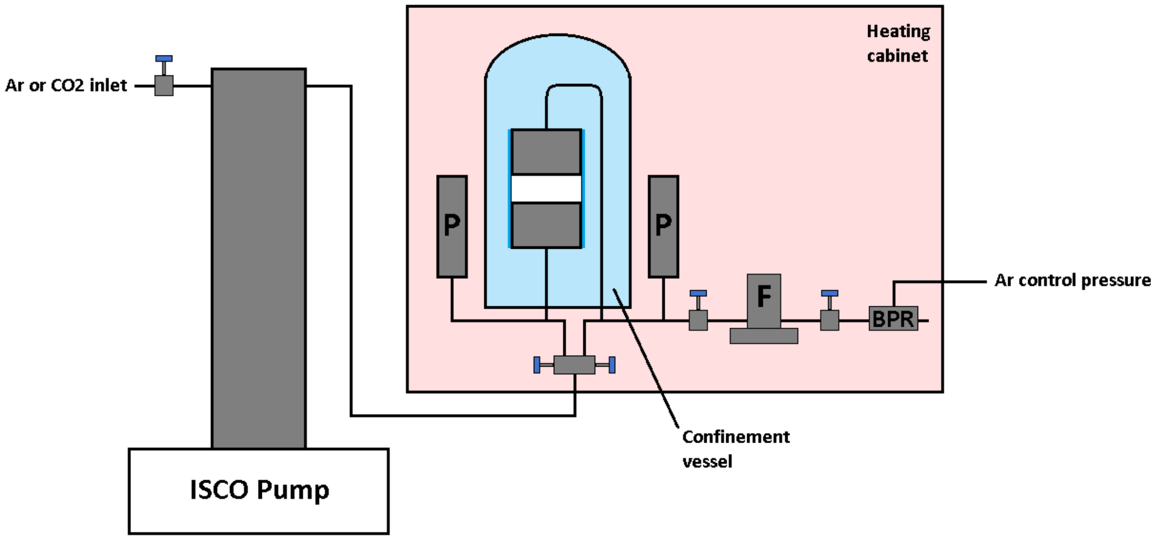

Figure 1 *Schematic drawing of the permeability apparatus used in the reported measurements. The Pump used is an ISCO 100DX.*

Sample permeabilities were first measured on dry samples, using Ar or CO_2. Next, the samples were hydrated using demineralized water, and subsequently, permeabilities were measured again using CO_2. Sample 2 was hydrated inside the apparatus, by injecting ~1 g of water into the fluid leads, and then pressurizing the fluid leads, displacing the water into the sample. This was attempted for Sample 3 as well, but additional water was added to this sample by taking the sample assembly out of the vessel and injecting water directly into the assembly. The total amount of water added to Sample 3 was estimated to be about 0.85 g. Sample 4 was wetted outside the apparatus by injecting water directly into the sample assembly using a high pressure pump connected to the upstream piston, until water appeared at the other side. The total amount of water added to sample 4 in this manner was 2.31 g. After wet measurements, samples 3 and 4 were dried in the sample assembly but outside the apparatus. Sample 3 was dried at 80°C for four days, and sample 4 at 60°C for almost 15 days, until the assembly mass was below that of the initial measurements. After drying, the permeability of these samples was measured again.

Results and discussion

Figure 2 shows all measured permeabilities. Under dry conditions, the permeabilities of samples 2 and 4 were too high to measure (>10^{-16} m^2). In the case of sample 2, this is most likely due to transport along the contact between the clay sample and the steel ring. In sample 4, this is interpreted as the quartz grains forming a supporting network, with insufficient clay to fill all pore space, enabling rapid transport. Under wet conditions, the permeability of sample 2 became too low to measure (<10^{-21} m^2). This shows the effect of passive confinement, i.e. confinement that does not expand or contract with the sample. Here, hydration of the clay results in a reduction of the effective permeability of the sample-ring assembly by more than 5 orders of magnitude as clay swelling blocks transport pathways. Furthermore, long term (9 weeks) exposure to supercritical CO_2, even with an elevated upstream pressure (17.8 MPa, for a differential pressure across the sample of 10.3 MPa) did not result in any increase in permeability as might be caused by dehydration and resulting shrinkage.

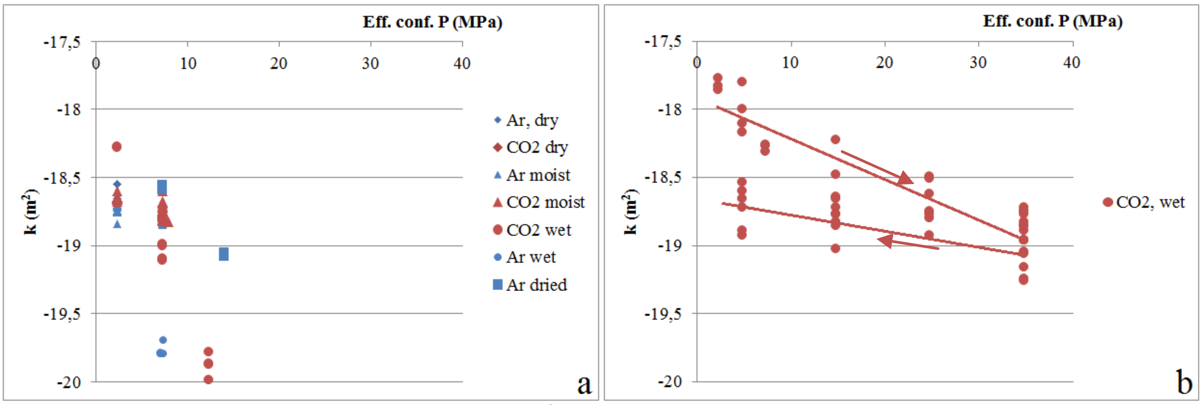

Figure 2 *Transient pulse permeabilities (m^2) plotted versus effective confining pressure (MPa), measured on: a) Sample 2; a pure smectite tablet, subsequently tested dry, moist, wet, and dried. b) Sample 4; a quartz-smectite tablet measured wet (as the dry permeability was too high to measure). The trend lines show the change in permeability with increasing and decreasing confinement, as indicated by the arrows.*

For samples under dynamic confinement, both confining pressure and water content influence permeability. The measurements on sample 3 and 4 show the sensitivity of the permeability of our tablets to effective confining pressure, which is similar to that of natural shale. Furthermore, it shows that under dynamic confinement (i.e. with a jacket that transmits a constant confining pressure, independent of changes in sample volume), and for a pure smectite sample, hydration leads to a stronger dependence of permeability on effective confining pressure, but this results in only a minor decrease in permeability of ~1 order of magnitude at an effective confining pressure of 12.3 MPa. However, it is not clear whether this is an effect of clay swelling, or whether the inhibition of flow through the pore network due to the presence of water also influenced permeability.

Finally, the measurements on sample 4 show that when the microstructure of the rock provides an unyielding, stress-supporting framework, this can have a strong impact on permeability, and specifically on the sensitivity of permeability to effective confining pressure and clay swelling effects. In the dry sample, the volume of clay is insufficient to fill the porosity, leading to a very high permeability (>10^{-16} m^2). When the sample is hydrated, smectite swelling and two phase flow effects lead to a permeability decrease in excess of 2 orders of magnitude. However, the permeability still remains higher than the permeability of a pure smectite sample by about 1.5 orders of magnitude. In addition, the permeability of the hydrated sample shows a weaker dependence on the effective confining pressure than the hydrated smectite sample. Upon decreasing the effective confining pressure on sample 4, the permeability only partly recovered, indicating that part of the observed decrease was due to non-elastic mechanisms.

Sample 3 was exposed to a constant CO_2 flow (interrupted only to restroke the ISCO pump) of 0.04 g/min for 45 days. This did not result in any significant change in permeability. After the hydrated samples 3 and 4 were dried outside the pressure vessel, permeabilities returned to original, pre-hydration values, indicating that hydration and subsequent compaction did permanently alter the sample microstructure.

Conclusions

The observed differences between dynamically and passively confined samples are of major importance when assessing the potential effects of clay swelling or shrinkage on shale caprock integrity. Under passive confinement, clay swelling or shrinkage can have a major impact on shale permeability. However, a 9 week exposure to dry supercritical CO_2 did not result in any changes in permeability in our small sample. Under dynamic confinement conditions, i.e. where the confinement can shift to compensate for the expansion or shrinkage, keeping effective confinement pressure rather than rock volume constant, the effect of hydration on permeability was much smaller, limited to less than an order of magnitude. Here, also, a near-continuous 45 day exposure to a dry CO_2 flow did not result in any significant enhancement of permeability.

A second important factor influencing the dependence of shale permeability on effective confining pressure and hydration is the shale mineral composition and/or microstructure. Sample 4, containing 69% quartz and 31% smectite, sufficient quartz to form a load-supporting grain network with smectite filling only part of the pore volume, showed a much greater decrease in permeability as a result of hydration than sample 3 (pure smectite). Furthermore, when hydrated, sample 4 shows a weaker decrease in permeability with increasing confining pressure than sample 3. Finally, overall permeabilities of sample 4 remain higher than those of sample 3.

We did not observe any increases in sample permeability resulting from dehydration due to exposure to dry supercritical CO_2. This observation, combined with the limited effects of swelling on permeability for dynamically confined samples suggests that overall, and on longer time scales, dehydration-induced shrinkage may not be an important leakage mechanism.

Acknowledgements
This research was funded by FME SUCCESS (grant 193825/S60 from the Research Council of Norway), as well as internal IFE funding.

References

Busch, A., Bertier, P., Gensterblum, Y., Rother, G., Spiers, C.J., Zhang, M., Wentinck, H.M. [2016] On sorption and swelling of CO_2 in clays. Geomechanics and Geophysics for Geo-Energy and Geo-Resources , **2**, 111–130.

Chalmers G.R.L., Ross, D.J.K., Bustin, R.M. [2012] Geological controls on matrix permeability of Devonian Gas Shales in the Horn River and Liard basins, northeastern British Columbia, Canada. International Journal of Coal Geology, **103**, 120-131.

De Jong, S.M., Spiers, C.J., Busch, A. [2014] Development of swelling strain in smectite clays through exposure to carbon dioxide. International Journal of Greenhouse Gas Control, **24**, 149-161.

Dong, J.-J., Hsu, J.-Y., Wu, W.-J., Shimamoto, T., Hung, J.-H., Yeh, E.-C., Wu, Y.-H., Sone, Y.-H. [2010] Stress-dependence of the permeability and porosity of sandstone and shale from TCDP Hole-A. International Journal of Rock Mechanics and Mining Sciences, **47**, 1141-1157.

Ghanizadeh, A., Bhowmik, S., Haeri-Ardakani, O., Sanei, H., Clarkson, C.R. [2015] A comparison of shale permeability coefficients derived using multiple non-steady-state measurement techniques: Examples from the Duvernay Formation, Alberta (Canada). Fuel, **140**, 371-387.

Ilton, E.S., Schaef, H.T., Qafoku, O., Rosso, K.M., Felmy, A.R. [2012] In Situ X-ray Diffraction Study of Na^+ Saturated Montmorillonite Exposed to Variably Wet Super Critical CO_2. Environmental Science & Technology, **46**, 4241-4248.

Schaef, H.T., Ilton, E.S., Qafoku, O., Martin, P.F., Felmy, A.R., Rosso, K.M. [2012] In situ XRD study of Ca^{2+} saturated montmorillonite (STX-1) exposed to anhydrous and wet supercritical carbon dioxide. International Journal of Greenhouse Gas Control, **6**, 220-229.
Van Noort, R., Yarushina, V. (2016) Water and CO_2 permeability of a shale sample core from Svalbard. Energy Procedia, **97**, 67-74.

Wang, L.L., Bornert, M., Héripré, E., Yang, D.S., Chanchole, S. [2014] Irreversible deformation and damage in argillaceous rocks induced by wetting/drying. Journal of Applied Geophysics, **107**, 108-118.